Supplementary Information

Section 1. Density of states

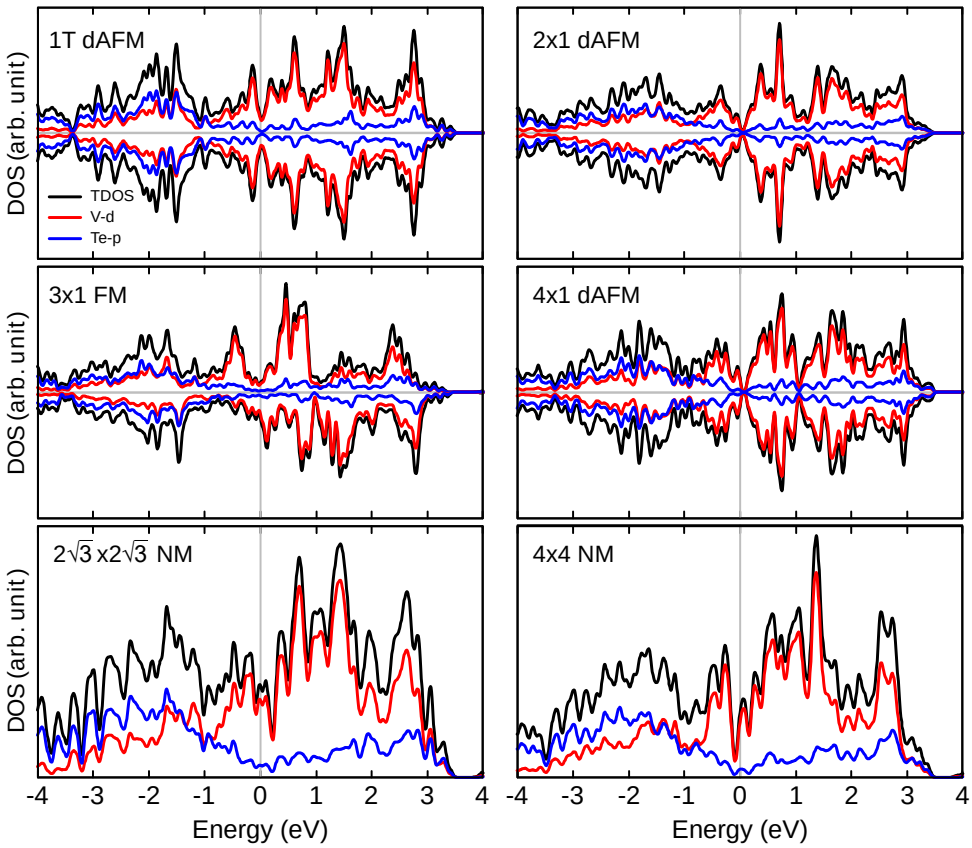

Fig. S1. The calculated density of states (DOS) for the most stable spin configuration of each CDW structure. The total, V-d, and Te-p projected DOS is represented by black, red, and blue lines, respectively. For magnetic solutions, we present the up-spin and down-spin DOS in the upper and lower panels, respectively. The Fermi energy is set to zero.

The calculated total and projected density of states (DOS) are presented in Fig.S1 where the V-d and Te-p states are represented in red and blue colors, respectively. For the given CDW structural phases, the most stable magnetic configurations are presented. The V-d states are mainly residing at -3.37– -3.54 eV while Te-p is in the range of -5.36 – 0.05 eV. It is interesting to note that the near-E_F states are significantly suppressed in the case of the AFM ground state. In the case of 2×1 and 4×1, the systems become insulating.

Section 2. Spin density plot

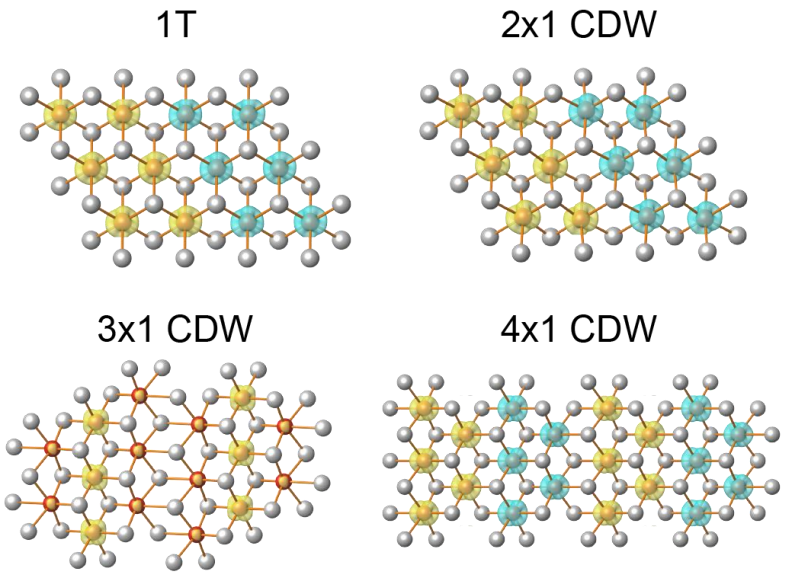

Fig. S2. The calculated spin density plots correspond to the four different CDW phases. The red- and gray-colored spheres represent V and Te atoms, respectively. The up and down spin densities are indicated by yellow- and cyan-colored isosurfaces with the isosurface value of 0.1 electrons per $Å^3$.

Figure S2 presents the calculated spin density plots for the most stable configurations at each structural phase. It is clear that the V ion is mainly responsible for magnetic moments. In 1T, 2×1, and 4×1 CDW phases, spin densities are equally distributed at V ions while, in the ferromagnetic 3×1 CDW, the magnetic moments mainly reside in the center of the 3×1 ribbon as in a previous bulk study [Ref. 18 of the main manuscript]. It is found that Te ions carry a moment smaller than ~0.1 μ_B.

Section 3. Total energy of magnetic 3×1 CDW phase

Figure S3 shows the calculated total energy of 3×1 phase in comparison to 1T, 2×1, and 4×1. Most stable is the FM order and AFM order is not stably converged. The energy difference between 3x1 and 4×1 is 28.6 meV/VTe_2.

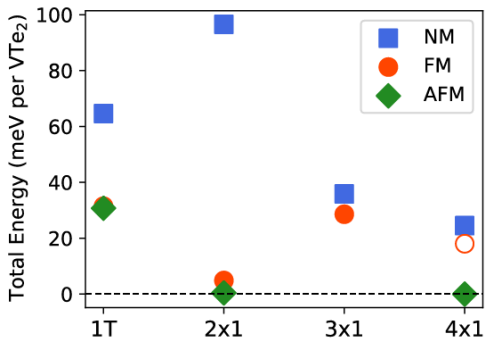

Fig. S3. The calculated total energies of nonmagnetic (blue squares), FM (red circles), and AFM (green diamonds) phase with respect to the most stable one. The open red circle for the 4×1 structure indicates that the converged solution is not FM but ferrimagnetic carrying the net magnetic moment of 0.29 μ_B per unit cell.

Section 4. Magnetic moments

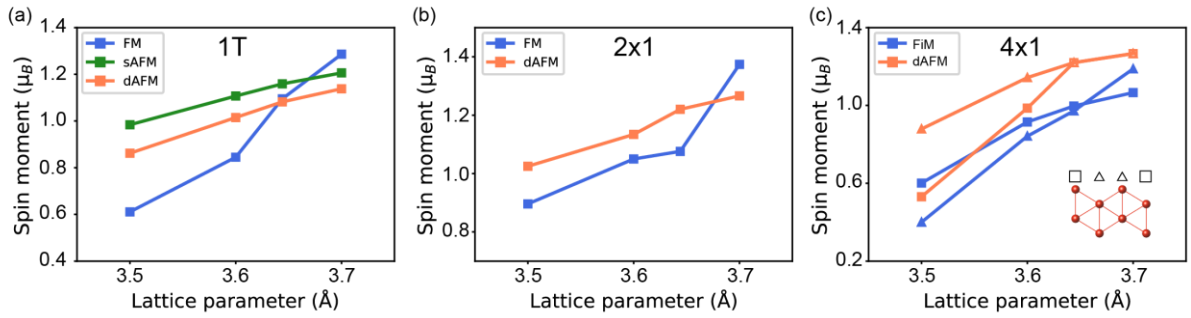

Fig. S4. The V spin moments for (a) 1T, (b) 2×1, and (c) 4×1 CDWs. In the 4×1 CDW, two different magnetic sites are presented; i.e., the inner and outer sites of the 4×1 ribbon are represented by the triangular and the square symbols, respectively. Note that dAFM (↑-↑-↓-↓ configuration) converges to the 2×1 structure for a ≥ 3.644 Å.

The calculated V spin moments are presented in Fig. S4 as a function of the lattice parameter. It is observed that the more (tensile) strain induces the larger moments, and the increasing feature is more rapid in the case of FM order. At a=3.7 Å, the FM moment size becomes largest in 1T and 2×1 CDW structures. Interestingly, the ground state configurations change accordingly. For the case of 4×1 CDW, the size of the moment is still enlarged while ferri- and antiferro-magnetic (no FM) phase are found to be stable.

Section 5. Uniaxial strain results

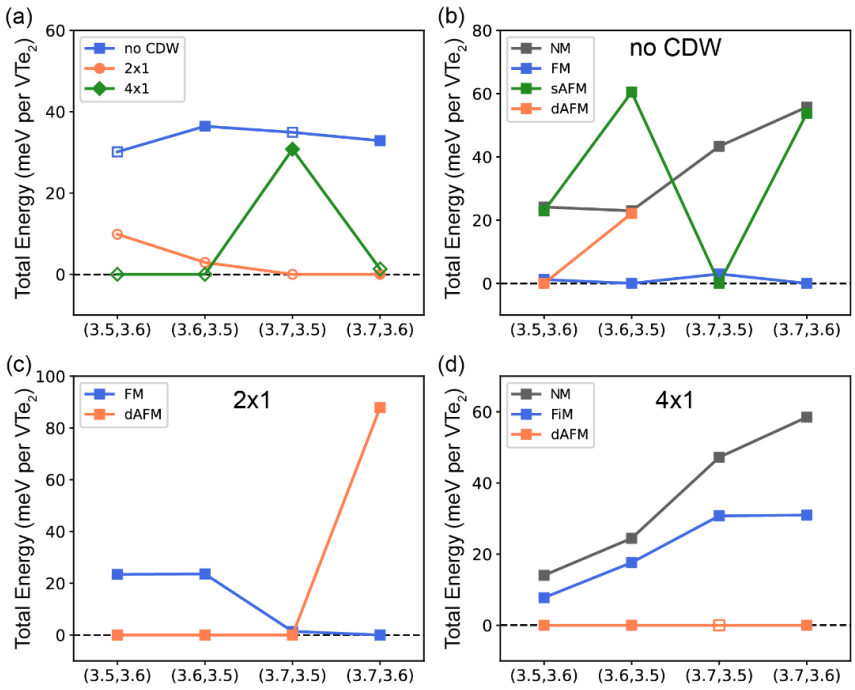

Fig. S5. (a) The calculated total energy of four different lattice parameters. The two numbers in the x labels correspond to the (a, b) lattice parameter. The ferromagnetic chain for AFM configuration is aligned along the b-axis. The structure is optimized for each lattice parameter with magnetic configurations. The filled symbols indicate FM or FiM states while the unfilled AFM. (b) The calculated total energy of the structure with no CDW distortion. This structure is different from 1T (P-3m1) due to the broken symmetry of a- and b- lattice parameters. The dAFM does not converge at (a, b) = (3.7, 3.5) and (3.7, 3.6) Å. (c) The calculated total energy for the 2×1 CDW. (d) The calculated total energy for the 4×1 CDW. The unfilled square of dAFM at (a, b) = (3.7, 3.5) Å converges to 2×1 while dAFM order is maintained.

Even though there is no experimental report of uniaxial strain for monolayer VTe_2, it would be interesting to investigate its effect. The total energy calculation results are presented in Fig. S4. We considered the 4 different configurations of (a, b) = (3.5, 3.6), (3.6, 3.5), (3.7, 3.5), and (3.7, 3.6) Å. The ferromagnetic chain for AFM configuration is aligned along the b-axis (the antiferromagnetic propagation vector is along the a-axis). In this calculation, the angle between a- and b-axes is fixed by 120°. Overall, the effects are similar to those of the biaxial strain shown in the manuscript. At the tensile of (a, b) = (3.5, 3.6) and (a, b) = (3.6, 3.5), the dAFM 4×1 CDW is the ground state. For the longer a-axis lattice parameter for (a, b) = (3.7, 3.5), the 2×1 CDW is stable with the dAFM spin order. However, to achieve the FM ground state, a small tensile strain along the b-axis is needed; at (a, b) = (3.7, 3.6), FM 2×1 CDW is most stable.